

Exendin-4 increases oxygen consumption and thermogenic gene expression in muscle cells

Jin-Seung Choung^{1,2,*}, Young-Sun Lee^{2,*} and Hee-Sook Jun^{1,2,3}

¹College of Pharmacy and Gachon Institute of Pharmaceutical Science, Gachon University, Incheon, Republic of Korea

²Lee Gil Ya Cancer and Diabetes Institute, Gachon University, Incheon, Republic of Korea

³Gachon Medical Research Institute, Gil Hospital, Incheon, Republic of Korea

* (J-S Choung and Y-S Lee contributed equally to this work)

Correspondence should be addressed to H-S Jun
Email
hsjun@gachon.ac.kr

Abstract

Glucagon-like peptide-1 (GLP1) has many anti-diabetic actions and also increases energy expenditure *in vivo*. As skeletal muscle is a major organ controlling energy metabolism, we investigated whether GLP1 can affect energy metabolism in muscle. We found that treatment of differentiated C2C12 cells with exendin-4 (Ex-4), a GLP1 receptor agonist, reduced oleate:palmitate-induced lipid accumulation and triglyceride content compared with cells without Ex-4 treatment. When we examined the oxygen consumption rate (OCR), not only the basal OCR but also the OCR induced by oleate:palmitate addition was significantly increased in Ex-4-treated differentiated C2C12 cells, and this was inhibited by exendin-9, a GLP1 receptor antagonist. The expression of uncoupling protein 1 (UCP1), β_3 -adrenergic receptor, peroxisome proliferator-activator receptor α (PPAR α) and farnesoid X receptor mRNA was significantly upregulated in Ex-4-treated differentiated C2C12 cells, and the upregulation of these mRNA was abolished by treatment with adenylate cyclase inhibitor (2'5'-dideoxyadenosine) or PKA inhibitor (H-89). As well, intramuscular injection of Ex-4 into diet-induced obese mice significantly increased the expression of UCP1, PPAR α and p-AMPK in muscle. We suggest that exposure to GLP1 increases energy expenditure in muscle through the upregulation of fat oxidation and thermogenic gene expression, which may contribute to reducing obesity and insulin resistance.

Key Words

- ▶ glucagon-like peptide-1 receptor agonist
- ▶ energy expenditure
- ▶ fat oxidation
- ▶ UCP1
- ▶ muscle

Journal of Molecular Endocrinology (2017) 58, 79–90

Introduction

Glucagon-like peptide-1 (GLP1) is an incretin hormone that is secreted from enteroendocrine gastrointestinal L cells after meal (Layer *et al.* 1995). GLP1 controls glucose homeostasis in many organs; it has a glucose-dependent insulinotropic effect, inhibits glucagon secretion, delays gastric emptying and reduces food intake and body weight (Drucker 2006). In addition, GLP1 is known to have beneficial effects on fatty liver

disease (Ding *et al.* 2006) and cardioprotective and neuroprotective effects (Liu *et al.* 2010, Briyal *et al.* 2014). As well, GLP1 has been shown to affect energy metabolism. During hyperglycaemic clamping, GLP1 administration increased energy expenditure in humans (Shalev *et al.* 1997). In addition, intracerebroventricular administration of GLP1 increased the proportion of fat oxidation in lean and obese Zucker rats (Hwa *et al.* 1998).

Recently, it was reported that brown adipose tissue thermogenesis is controlled by central nervous system GLP1 receptor signaling (Lockie *et al.* 2012).

Obesity develops due to the imbalances between energy intake and energy expenditure. Therefore, promoting energy expenditure is an attractive strategy for combating obesity. In addition to the physical activity, adaptive thermogenesis is one component of energy expenditure that can be readily altered. Thermogenesis is regulated by sympathetic nervous system through peripheral tissues such as brown fat and skeletal muscle (Bal *et al.* 2012, Chechi *et al.* 2013).

We previously reported that treatment of *ob/ob* mice with recombinant adenoviruses expressing GLP1 (rAd-GLP1) decreased fat mass and increased energy expenditure, as analyzed by indirect calorimetry, compared with untreated mice fed equal amounts of food (Lee *et al.* 2012). We hypothesize that GLP1 might affect energy expenditure and fat oxidation in muscle, contributing to the improvement of insulin sensitivity seen after GLP1 treatment in these mice. In this study, we investigated whether the GLP1 receptor agonist, exendin-4 (Ex-4) increases energy expenditure and the expression of energy metabolism-related genes in mouse muscle cells *in vitro* and *in vivo*.

Materials and methods

Animals

C57BL/6 mice were obtained from the Korea Research Institute of Bioscience and Biotechnology (Daejeon, Korea) and were maintained at a facility at Gachon University. Male C57BL/6 mice (6 weeks old) were fed a high-fat diet (HFD; 60% kcal from fat) for 8 weeks. All animal experiments were carried out under a protocol approved by the Institutional Animal Care and Use committee at Lee Gil Ya Cancer and Diabetes Institute, Gachon University.

Materials

Cell culture media and fetal bovine serum (FBS) were purchased from WELGENE (Daegu, Korea) and horse serum from Gibco-BRL. Palmitate, oleate, bovine serum albumin, H-89, exendin-4, exendin-9, oligomycin, carbonil cyanide p-trifluoromethoxy phenylhydrazone (FCCP), rotenone and antimycin A were purchased from Sigma. 2'5'-dideoxyadenosine and LY294002 were products of Calbiochem.

Cell culture

C2C12 cells (mouse myoblasts) were cultured in DMEM medium supplemented with 10% (v/v) heat-inactivated fetal bovine serum, 25 mM glucose, 2 mM L-glutamine, 100 U/mL penicillin and 100 µg/mL streptomycin at 37°C in a humidified atmosphere containing 95% (v/v) air and 5% (v/v) CO₂. The cells were seeded at a density of 5.0 × 10⁵/well in 6-well plates. To induce the myogenic differentiation of C2C12 cells, the cells were cultured to 85% (v/v) confluence in differentiation media (DMEM with 2% (v/v) horse serum), which was changed daily for 4 days.

Oil Red O staining

Biochemical quantification of fat accumulation in Ex-4-treated C2C12 cells was assessed with the fat-soluble dye, Oil Red O. Differentiated C2C12 cells were pretreated with 20 nM Ex-4 for 24 or 48 h or 0, 10, 20 or 40 nM Ex-4 for 48 h, and then stimulated with 400 µM free fatty acid mixture at a 2:1 ratio of oleate to palmitate for 12 h. C2C12 cells were fixed with 10% (w/v) neutral buffered formalin for 30 min. The cells were stained with Oil Red O solution (Sigma, Oil Red O in 60% (v/v) isopropanol) for 30 min at room temperature. Stained cells were rinsed twice with distilled water and washed with isopropanol. Then, the optical absorbance of the sample containing a dye was read at 450 nm by VersaMax microplate reader (Molecular Devices).

Analysis of triglyceride content

Differentiated C2C12 cells were pretreated with 20 nM Ex-4 for 24 or 48 h or 0, 10, 20 or 40 nM Ex-4 for 48 h, and then stimulated with 400 µM oleate:palmitate mixture (2:1) for 12 h. Cells were lysed in ethanolic KOH (2 parts EtOH:1 part 30% (v/v) KOH) and incubated overnight at 55°C. The lysates were mixed with H₂O:EtOH (1:1) and centrifuged for 5 min. The supernatants were mixed with 1 M MgCl₂ and incubated for 10 min on ice. The samples were centrifuged for 5 min. The amount of triglyceride in supernatants was measured using a triglyceride assay kit (Asan Pharmaceutical Co. Ltd., Seoul, Korea). The absorbance was measured at 550 nm.

Analysis of free fatty acid (FFA) content

Differentiated C2C12 cells were treated with 20 nM Ex-4 for 24 or 48 h. The cells were extracted by homogenization

with 200 μ L of 1% (v/v) Triton X-100 in pure chloroform in a microhomogenizer. The lower phase was collected after centrifuging for 10 min at 9300g, and the chloroform was evaporated. The dried lipids were dissolved in 200 μ L of fatty acid assay buffer (BioVision). The amount of FFA was measured using a FFA quantification kit (K612-100, BioVision). The fluorescence was measured with a multi-label plate counter (Victor 3, Perkin Elmer) with excitation at 535 nm and emission at 590 nm.

Oxygen consumption rate (OCR) measurement

C2C12 cells were seeded at a density of 1.66×10^4 cells/well in 24-well XF plates in culture medium and cultured for 48 h at 37°C and 95% (v/v) air and 5% (v/v) CO₂. For differentiation, the media was replaced with differentiation media (DMEM with 2% (v/v) horse serum) every day for 4–6 days. Differentiated C2C12 cells were pretreated with or without 20 nM Ex-9 for 30 min and then treated with 20 nM Ex-4 for 48 h (changed medium and Ex-4 added every 24 h). For BSA conjugation, 20 mM palmitate or oleate in 0.01 M NaOH was incubated at 70°C for 30 min, and the palmitate or oleate was then mixed with 5% (v/v) BSA in PBS at a 3:1 molar ratio of BSA to palmitate or oleate. BSA-conjugated oleate and palmitate were mixed at a proportion of 2:1. Differentiated C2C12 cells were treated with the oleate:palmitate–BSA conjugated mixture at a final concentration of 200 μ M. Oxygen consumption was determined using Seahorse XF24 extracellular Flux analyzer (Seahorse Bioscience, North Billerica, MA, USA) as previously described (Schuh *et al.* 2012) with slight modifications. The oxygen consumption rate (OCR) measurements were obtained at baseline (3 \times (3 min mix, 2 min wait and 3 min measure)) and after injection of oleate:palmitate mixture (200 μ M) (5 \times (3 min mix, 2 min wait and 3 min measure)), oligomycin (1 μ M) (3 \times (3 min mix, 2 min wait and 3 min measure)), FCCP (1 μ M) (3 \times (3 min mix, 2 min wait and 3 min measure)) and rotenone (0.1 μ M)/antimycin A (2 μ M) (3 \times (3 min mix, 2 min wait and 3 min measure)) sequentially.

Immunoprecipitation

Differentiated C2C12 cells were treated with 20 nM Ex-4 for 72 h (Ex-4 added every 24 h). Mitochondria were isolated from Ex-4-treated C2C12 cells using a Thermo mitochondrial isolation kit (89874, Thermo Fisher). Soleus muscle tissue was homogenized with radioimmunoprecipitation assay (RIPA) buffer (50 mM Tris–HCl, pH 8.0; 150 mM NaCl; 0.1% (w/v) SDS, 0.5%

(w/v) Na-deoxycholate; 1% (v/v) NP-40; and a 1:100 dilution of protease inhibitor cocktail (P8340, Sigma-Aldrich)). Mitochondria (300 μ g protein) or soleus muscle lysates (600 μ g protein) were precleared by incubating for overnight with normal rabbit IgG and protein A/G PLUS-agarose beads (sc-2003, Santa Cruz Biotechnology) at 4°C in a rotary shaker. After centrifugation, supernatants were incubated overnight with anti-uncoupling protein (UCP)-1 antibody (14670, Cell Signaling Technology) at 4°C and then 20 μ L of protein A/G PLUS-agarose beads was added to the samples, and samples were incubated at 4°C on a rotating device overnight. After centrifugation, pellets were washed with RIPA buffer. These immunoprecipitated samples were used for SDS-PAGE and Western blot analysis with anti-UCP1 antibody (AB1426, Millipore).

Western blotting

Total cell lysates from undifferentiated or differentiated C2C12 cells, quadriceps muscle tissue or brown adipose tissue were prepared using Mammalian Protein Extraction Buffer (GE HealthCare) containing a protease and phosphatase inhibitor cocktail (Sigma-Aldrich). The isolated protein (30–50 μ g) was electrophoresed in a 10% (w/v) acrylamide–SDS gel and transferred to polyvinylidene difluoride membranes. After 1 h of blocking with 3% (w/v) skim milk, membranes were incubated with anti-phospho-AMP-activated protein kinase (AMPK) α (Thr172) (2535, Cell Signaling Technology), AMPK α (2532, Cell Signaling Technology), anti-phospho-acetyl-CoA carboxylase (ACC) (3661, Cell Signaling Technology), ACC (3676, Cell Signaling Technology), UCP1 (AB1426, Millipore), PGC1 α (ab 54481, Abcam), HSP60 (ab 46798, Abcam) or β -actin (sc-47778, Santa Cruz Biotechnology) antibody. Membranes were then incubated with horseradish peroxidase-conjugated goat anti-rabbit IgG (sc-2004, Santa Cruz Biotechnology) or goat anti-mouse IgG antibodies (sc-2005, Santa Cruz Biotechnology). Signals were detected with ECL detection kit (Millipore) and analyzed using a Luminescent Image Analyzer LAS4000 (Fuji Film, Tokyo, Japan).

RNA isolation and real-time quantitative PCR

Total RNA was isolated from cells using RNA iso Plus (TAKARA) according to the manufacturer's protocol. cDNA was synthesized from 2 μ g total RNA using the PrimeScript 1st-strand cDNA synthesis kit (TAKARA). Quantitative

real-time PCR (qRT-PCR) was performed using a reaction mixture containing SYBR Green master mix (TAKARA). PCR amplification was carried out in an ABI 7900HT Real-Time PCR Sequence Detection System at 50°C for 2 min and 95°C for 10 min, followed by 40 cycles of 95°C for 15 s and 60°C for 1 min. The sequences of the primer pairs are shown in Table 1.

Intracellular cAMP measurement

Differentiated C2C12 cells in 6-well plates were treated with 20 nM Ex-4. Media was removed and 1 mL of 0.1 M HCL was added to the cells. The cells were lysed by incubation for 20 min at room temperature. The lysate was centrifuged at 800g for 5 min to pellet the cellular debris, and the supernatant was assayed for determination of cAMP concentration using a cAMP ELISA kit (Enzo Life Sciences, Farmingdale, NY, USA).

In vivo experiment

HFD-induced obese mice were given an intramuscular injection of Ex-4 (1 µg/kg). At 12 h after Ex-4 treatment, the mice were killed by cervical dislocation and quadriceps muscle tissue was removed. HFD-induced obese mice or C57BL/6 male mice were given an intramuscular injection of Ex-4 (1 µg/kg/day) for 4 weeks. The mice were killed by cervical dislocation and soleus muscle tissue was removed for qRT-PCR and immunoprecipitation and Western blot analysis.

Statistical analysis

Data are presented as the mean ± S.E.M. Statistical analysis was performed using an unpaired parametric Student's *t*-test for two groups or ANOVA followed by Fisher's protected least significant difference test for multiple groups. *P* < 0.05 was accepted as significant.

Results

Ex-4 treatment reduced fatty acid-induced lipid accumulation in differentiated C2C12 cells

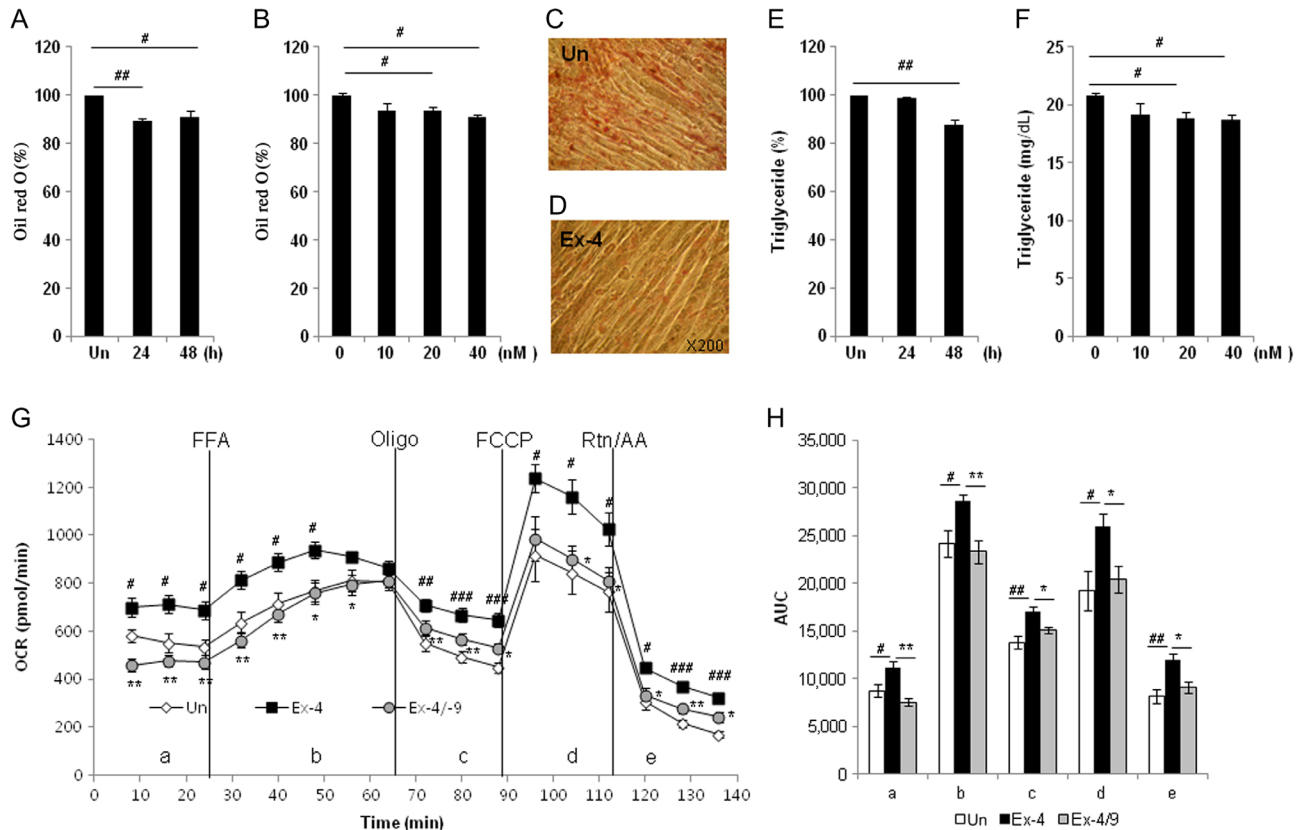
To investigate whether Ex-4 affects lipid accumulation in differentiated C2C12 cells, we treated the cells with oleate and palmitate at a proportion of 2:1 in the presence or absence of Ex-4, and Oil Red O staining was performed to determine fat accumulation. The Oil Red O content in the cells was significantly decreased by Ex-4 treatment at 24 and 48 h compared with untreated cells (Fig. 1A), and it was dose dependently decreased by Ex-4 treatment, reaching significance at 20 and 40 nM (Fig. 1B). Ex-4 decreased the lipid droplets in differentiated C2C12 cells (Fig. 1C and D). In addition, triglyceride content was significantly reduced in Ex-4-treated cells at 48 h compared with untreated cells (Fig. 1E), and it was also dose dependently decreased by Ex-4 treatment, reaching significance at 20 and 40 nM (Fig. 1F). These results indicated that Ex-4 reduced the intracellular lipid accumulation induced by fatty acid in muscle cells.

Ex-4 treatment increased OCR in differentiated C2C12 cells

As fat accumulation was reduced in C2C12 cells by Ex-4 treatment, we also measured energy expenditure. We treated differentiated C2C12 cells with Ex-4 for 48 h and then measured the basal OCR. The basal OCR was significantly increased in Ex-4-treated C2C12 cells compared with untreated cells. In addition, we examined OCR after oleate:palmitate addition and found that Ex-4 treatment also significantly increased oleate:palmitate-induced OCR compared with the untreated group. We then measured OCR for ATP turnover and proton leak after treatment with oligomycin, an ATP synthase inhibitor. Ex-4 treatment displayed significantly higher proton

Table 1 List of qRT-PCR primers and sequences.

Primer	Sense	Anti-sense
Cyclophilin	5'-TGGAGAGCACCAAGACAGACA-3'	5'-TGCCGGAGTCGACAATGAT-3'
UCP1	5'-CTGGGCTTAACGGGTCCTC-3'	5'-CTGGGCTAGGTAGTGCCAGTG-3'
UCP2	5'-GACCTCCCTTGCCACTTCAC-3'	5'-GAAGGCATGAACCCCTTGAG-3'
UCP3	5'-CCGATACATGAACGCTCCC-3'	5'-AAGCTCCCAGACGCAGAAAG-3'
PPAR-α	5'-TATTCGGCTGAAGCTGGTGTAC-3'	5'-CTGGCATTGTCCGGTCT-3'
FXR	5'-GACAGCGAAGGGCGTGAC-3'	5'-TTCCGTTTTCTCCCTGAAA-3'
β ₃ -ar	5'-CGCTACCTAGCTGTACCAA-3'	5'-TAGAAGGAGACGGAGGAGGA-3'
CPT1	5'-CAAAGATCAATCGGACCCTAGAC-3'	5'-CGCCACTCAGATGTTCTTC-3'
HSL	5'-GGTGACACTCGAGA AGACAA TA-3'	5'-GCCGCCGTGCTGTCTCT-3'

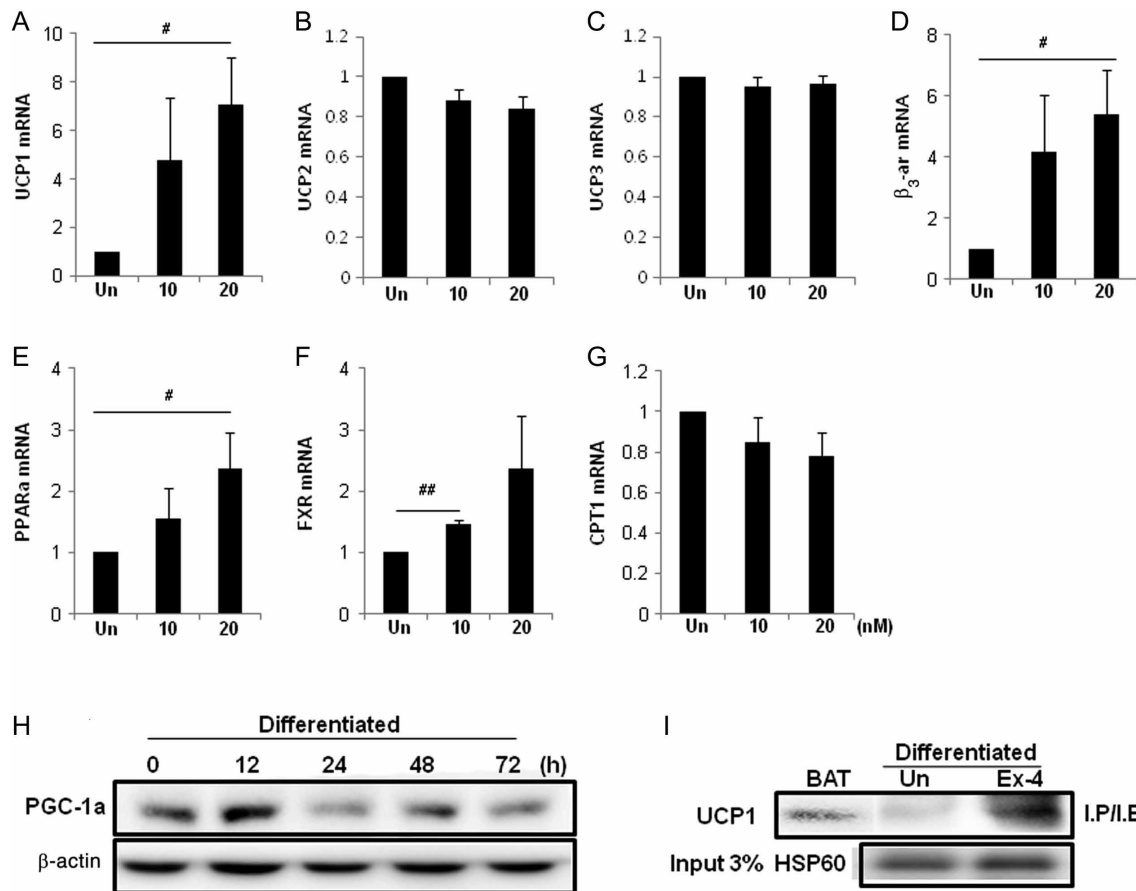
**Figure 1**

Ex-4 reduced fatty acid-induced lipid accumulation and increased oxygen consumption rate in differentiated C2C12 cells. (A and E) Differentiated C2C12 cells were pretreated without or with 20 nM Ex-4 for 24 or 48 h, and then stimulated with 400 μ M free fatty acid mixture at a 2:1 ratio of oleate to palmitate for 12 h. (B and F) Differentiated C2C12 cells were pretreated without or with 10, 20 or 40 nM Ex-4 for 48 h, and then stimulated with 400 μ M free fatty acid mixture for 12 h. (A and B) Lipid content was detected by a quantitative Oil Red O dye method. Data are percentages of Oil Red O dye content relative to untreated (Un) cells. (C and D) Differentiated C2C12 cells were pretreated without or 40 nM Ex-4 for 48 h, and then stimulated with 400 μ M free fatty acid mixture for 12 h. The cells were stained with Oil Red O. Lipid droplets in C2C12 cells were observed by microscope (200 \times). (E and F) Total triglyceride content was measured in C2C12 cells. Data are presented as mean \pm s.e.m. * P < 0.05, ** P < 0.005 compared with untreated group. (G) Differentiated C2C12 cells were pre-treated with or without 20 nM Ex-4 for 30 min and then treated with Ex-4 for 48 h. Oleate and palmitate at a proportion of 2:1 (200 μ M), oligomycin (Oligo), FCCP and rotenone with antimycin A (Rtn/AA) were added at the indicated times (lines) and OCR was measured over 136 min. (H) The area under the curve (AUC) was calculated. n = 3–5, mean \pm s.e.m. * P < 0.05, ** P < 0.01, *** P < 0.005 compared with untreated group (Un) and ** P < 0.05, * P < 0.01 compared with the Ex-4-treated group.

leak-associated OCR compared with untreated cells. Carbonyl cyanide-4-(trifluoromethoxy) phenylhydrazone (FCCP) addition uncouples the transport of electrons from ATP production and results in maximal respiration. In Ex-4-treated cells, maximal respiration was significantly increased after FCCP addition. Lastly, rotenone and antimycin A, inhibitors of complex I and III, were added to shut down the electron transfer, revealing the non-mitochondrial respiration. Ex-4-treated cells were increased from untreated cells after rotenone and antimycin treatment. These effects were inhibited by Exendin-9 (9-39), a GLP1 receptor antagonist (Fig. 1G and H). These results suggest that Ex-4 increased not only basal OCR, but also fatty acid-induced OCR by increasing uncoupling efficiency and proton leak in muscle cells.

Ex-4 treatment increased mRNA and protein expression of thermogenic genes in differentiated C2C12 cells

As Ex-4 treatment significantly increased oxygen consumption in C2C12 cells, we first determined mRNA expression of UCP1, UCP2 and UCP3 in Ex-4-treated differentiated C2C12 cells. The expression of UCP1 mRNA was upregulated at 24 h after 20 nM of Ex-4 treatment (Fig. 2A); however, the expression of UCP2 and UCP3 mRNA was not changed (Fig. 2B and C). As UCP1 expression is induced by β_3 -adrenergic receptor activation (Mattsson *et al.* 2011), we examined mRNA expression of β_3 -adrenergic receptor. As shown in Fig. 2D, the expression of β_3 -adrenergic receptor mRNA was significantly increased in differentiated C2C12 cells by 20 nM of Ex-4 treatment.

**Figure 2**

Ex-4 increased the expression of thermogenic gene mRNA and protein in differentiated C2C12 cells. Differentiated C2C12 cells were treated with 10 or 20 nM Ex-4 for 24 h. The expression of (A) UCP1, (B) UCP2, (C) UCP3, (D) β_3 -adrenergic receptor (β_3 -ar), (E) PPAR α , (F) FXR and (G) CPT1 mRNA was measured by qRT-PCR. The fold change was calculated as the ratio of the expression level in untreated (Un) cells. Results are representative of 4 independent experiments. Data are means \pm s.e.m. * P < 0.05, ** P < 0.01 compared with untreated cells. (H) Protein expression of PGC1 α was measured by Western blot. Differentiated C2C12 cells were treated with Ex-4 20 nM for 0, 12, 24, 48 and 72 h (Ex-4 added every 24 h). Differentiated C2C12 cells were loaded with 50 μ g of total whole lysate. β -actin was a loading control. (I) Mitochondria isolated from differentiated C2C12 cells, which were treated with 20 nM Ex-4 for 72 h (added per 24 h). Mitochondria lysates were immunoprecipitated (IP) with anti-UCP1 (14670, Cell Signaling) antibody and immunoblotted (IB) with anti-UCP1 (AB1426, Millipore) antibody. Mouse brown adipose tissue (BAT) protein (2 μ g) was loaded as a positive control for UCP1 and input 3% (w/w) mitochondria protein was loaded and HSP60 was a loading control for IP.

In addition, we examined the expression of upstream molecules related to fat oxidation and thermogenesis such as PPAR α , farnesoid X receptor (FXR), carnitine palmitoyltransferase (CPT)-1 and peroxisome proliferator-activated receptor γ coactivator (PGC)-1 α . The expression of PPAR α mRNA and FXR mRNA was significantly increased after 20 or 10 nM of Ex-4 treatment, respectively (Fig. 2E and F). However, the CPT1 mRNA expression levels were not significantly changed (Fig. 2G). The protein level of PGC1 α was increased by Ex-4 treatment (Fig. 2H). In addition, we observed that the protein expression of UCP1 was increased after Ex-4 treatment in differentiated C2C12 cells. Because UCP1 is primarily expressed in the mitochondria of brown adipose tissue, but not in muscle

(Ricquier & Bouillaud 2000), we confirmed this result in isolated mitochondria by immunoprecipitation and Western blot analysis, respectively. We found that UCP1 protein expression was clearly increased by Ex-4 treatment (Fig. 2I).

Ex-4 treatment increased the expression of hormone-sensitive lipase (HSL) mRNA and decreased FFA concentration in differentiated C2C12 cells

FFAs are required to activate UCP1 for thermogenesis (Hagen & Lowell 2000). Therefore, we measured the expression of adipose triglyceride lipase and HSL mRNA in Ex-4-treated C2C12 cells. The expression of adipose

triglyceride lipase was not detectable in C2C12 cells, but the expression of HSL mRNA was significantly increased in Ex-4-treated C2C12 cells (Fig. 3A). We also measured the concentration of FFA in Ex-4-treated C2C12 cells. The FFA content in Ex-4-treated cells was not significantly different from untreated cells after 24 or 48 h of treatment. However, the concentration of FFA in Ex-4-treated C2C12 cells was significantly decreased at 48 h compared with 24 h (Fig. 3B). These results suggest that Ex-4 treatment increases fatty acid utilization.

Ex-4 upregulates mRNA expression of thermogenic genes via cAMP/PKA signaling pathways in differentiated C2C12 cells

The function of both GLP1 and Ex-4 are mediated via the activation of cAMP/protein kinase (PK)A and transactivation of the epidermal growth factor receptor leading to the activation of phosphatidylinositol-3 kinase (PI3K) signaling pathways (Lee & Jun 2014). To investigate whether the changes of expression of thermogenic genes by Ex-4 treatment is affected by these signaling pathways, we first measured cAMP production levels in Ex-4-treated differentiated C2C12 cells. We found that cAMP production was significantly increased at 10 min after Ex-4 treatment in C2C12 cells compared with untreated cells (Fig. 4A).

PKA is activated depending on cellular levels of cAMP. Thus, we pretreated differentiated C2C12 cells with an adenylate cyclase inhibitor (2'5'-dideoxyadenosine) or PKA inhibitor (H-89) and determined the expression levels of UCP1, β_3 -adrenergic receptor, PPAR α and FXR mRNA after Ex-4 treatment. The expression of UCP1,

β_3 -adrenergic receptor, PPAR α and FXR mRNA was increased by Ex-4; however, it was inhibited by adenylate cyclase (Fig. 4B, E, H and K) or PKA (Fig. 4C, F, I and L) inhibitors. In addition, we pretreated differentiated C2C12 cells with a PI3K inhibitor (LY294002). However, pretreatment with a PI3K inhibitor did not inhibit the induction of UCP1, β_3 -adrenergic receptor or PPAR α mRNA expression, except for FXR mRNA (Fig. 4D, G, J and M). This suggests that Ex-4 induced the expression of UCP1, β_3 -adrenergic receptor, PPAR α and FXR mRNA via activation of cAMP and PKA signaling.

AMPK activation stimulates fatty acid oxidation in skeletal muscle (Winder & Hardie 1999). Thus, we examined the protein levels of AMPK and phosphorylated AMPK in Ex-4-treated differentiated C2C12 cells. The expression of phosphorylated AMPK was increased at 3 h after Ex-4 treatment compared to the untreated cells, but levels of AMPK were not changed. In addition, phospho-AMPK expression is associated with phospho-ACC (Choudhury *et al.* 2014). Thus, we investigated the expression of ACC and phosphorylated ACC in Ex-4-treated C2C12 cells. The expression of the phospho-ACC was increased at 3 h after Ex-4 treatment (Fig. 4N).

Injection of Ex-4 increased UCP1, PPAR α and p-AMPK protein in muscle tissue of mice

To examine whether Ex-4 shows similar effects on muscle tissue *in vivo*, Ex-4 (1 μ g/kg) was given by intramuscular injection to HFD-induced obese C57BL/6 mice. The mice were killed at 12 h after Ex-4 injection, and quadriceps muscle tissue was harvested for Western blotting. The expression of PPAR α and p-AMPK protein was significantly increased in quadriceps muscle of Ex-4-injected mice compared with untreated control mice (Fig. 5A, B and C). In addition, we examined the expression of UCP1 in regular chow-fed or HFD-fed C57BL/6 mice after Ex-4 treatment. Soleus muscle (98% type I fibers) is rich in mitochondria; thus, we used the soleus muscle to investigate the UCP1 alteration in muscle by Ex-4 treatment. We confirmed the significant increase of UCP1 mRNA and protein expression in soleus muscle tissue by treatment with Ex-4 (1 μ g/kg/day) for 4 weeks (Fig. 5D, E and F).

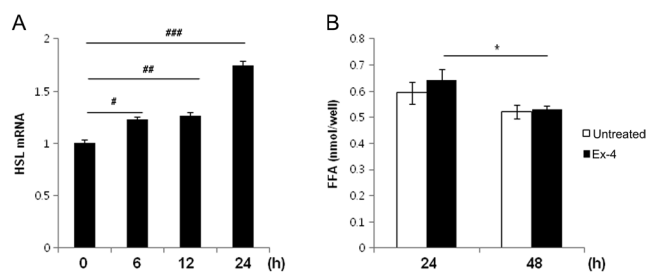
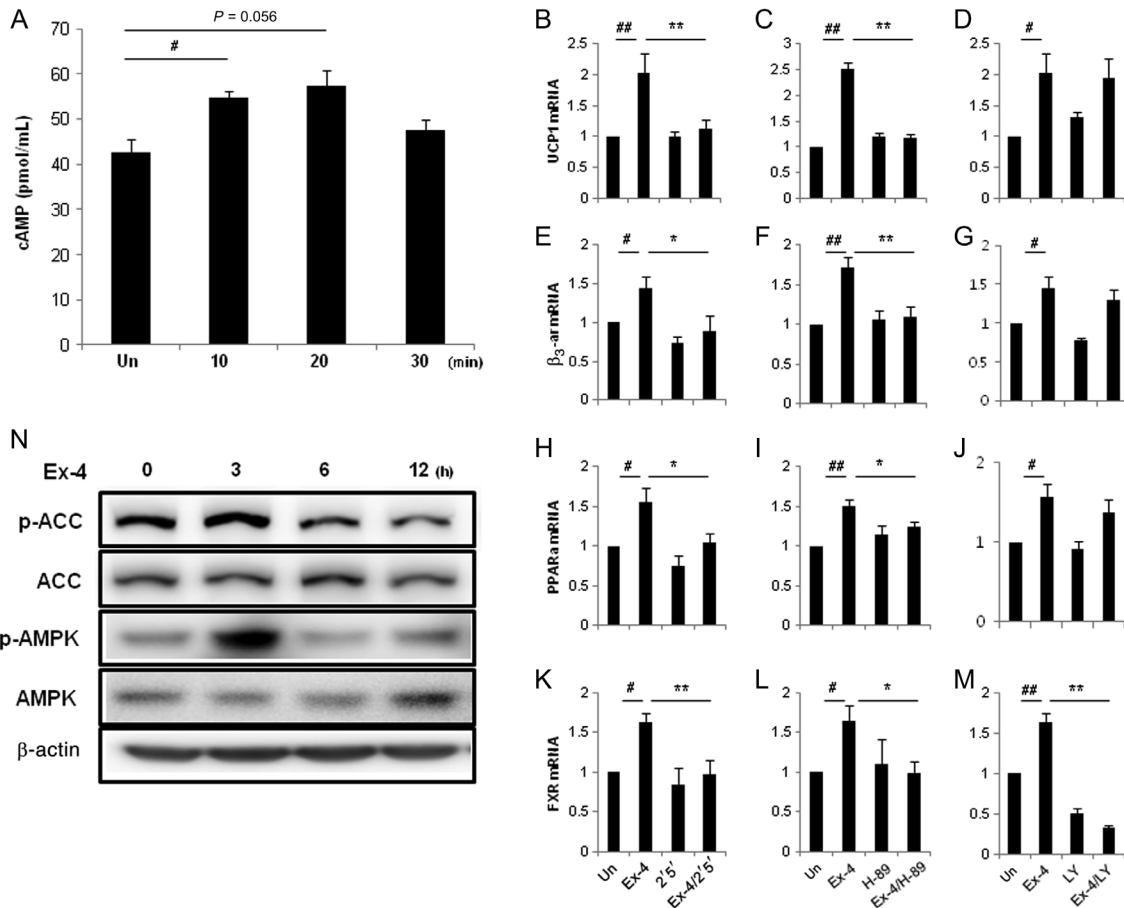


Figure 3

Expression of HSL mRNA and the concentration of free fatty acid in Ex-4-treated C2C12 cells. (A) Differentiated C2C12 cells were treated with Ex-4 20 nM for 0, 6, 12 or 24 h. The expression of HSL mRNA was measured by qRT-PCR. The fold change was calculated as the ratio of the expression level at 0 h. (B) Differentiated C2C12 cells were treated with Ex-4 20 nM for 24 or 48 h. The concentration of FFA was measured in Ex-4-treated C2C12 cells. $N=6$. Data are means \pm S.E.M. * $P < 0.01$, ** $P < 0.005$, *** $P < 0.001$ compared with 0 h, and * $P < 0.05$ compared with Ex-4 treated.

Discussion

Muscle is an important organ for controlling insulin resistance and energy metabolism. In skeletal muscle, insulin resistance has been linked to lipid accumulation and a defect in fatty acid metabolism, which includes

**Figure 4**

Ex-4 regulates the thermogenic gene expression via cAMP/PKA signaling pathways in differentiated C2C12 cells. (A) Intracellular cAMP production was measured at 10-min intervals after Ex-4 treatment. Results are representative of 3 independent experiments. $^{\#}P < 0.05$ compared with untreated group. (B, C, D, E, F, G, H, I, J, K, L and M) Differentiated C2C12 cells were pre-treated with 2'5'-dideoxyadenosine (2'5'; 50 μ M for 30 min), H-89 (1 μ M for 30 min) or LY294002 (LY; 4 μ M for 3 h) and then treated with Ex-4 (20 nM for 24 h). The expression of UCP1, β_3 -adrenergic receptor (β_3 -ar), PPAR α and FXR mRNA was measured by qRT-PCR. The fold change was calculated as ratio of the expression level in untreated cells. $^{\#}P < 0.05$, $^{\#\#}P < 0.01$ compared with untreated group and $^*P < 0.05$, $^{**}P < 0.01$ compared with the Ex-4-treated group. Results are representative of 4–6 independent experiments. (N) The cells were treated with Ex-4 (20 nM) and harvested at the indicated times. The expression of p-AMPK, AMPK, p-ACC and ACC protein was measured by Western blot. β -actin was analyzed as a loading control.

alterations in fatty acid uptake, triacylglycerol synthesis and fatty acid oxidation. In addition, skeletal muscle, along with brown adipose tissue, is important in non-shivering thermogenesis, which may increase energy expenditure to combat obesity (Bal *et al.* 2012).

GLP1 shows beneficial effects on the reduction of obesity and improvement of insulin sensitivity. In a previous study, we found that GLP1-treated mice showed reduced fat mass and increased energy expenditure compared with untreated mice fed equal amounts (Lee *et al.* 2012). Therefore, in this study, we investigated whether Ex-4, a GLP1 receptor agonist, improves energy metabolism in muscle. We found that Ex-4 significantly decreased lipid and triglyceride content and also increased basal and fat-induced OCR in differentiated C2C12 cells.

These results indicate that acute exposure to Ex-4 reduces intracellular lipid via an increase of energy expenditure in muscle.

Basal energy expenditure is required to maintain the body's normal metabolic activity, i.e. maintenance of body temperature (Corpeleijn *et al.* 2009). Non-shivering thermogenesis, which mainly depends on thermogenic metabolism, is an important function of energy expenditure (Terrien *et al.* 2010). Thus, thermogenesis can improve energy expenditure and fat oxidation in muscle. Mitochondrial uncoupling proteins (UCPs) are mitochondrial anion carrier proteins expressed in the inner mitochondrial membrane (Fisler & Warden 2006). UCP1 plays an important role in energy expenditure and regulation such as thermogenesis in mitochondria

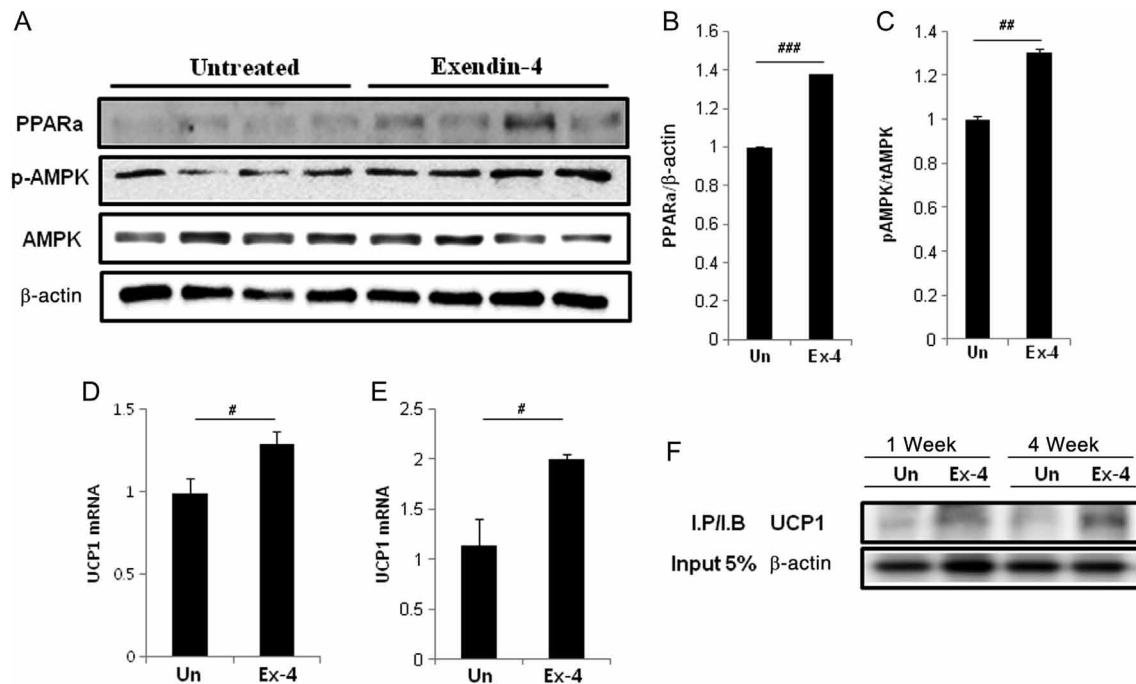


Figure 5

Intramuscular injection of Ex-4 increased UCP1, PPAR α and p-AMPK protein in muscle of HFD-induced obesity mice or regular chow diet-fed mice. Ex-4 (1 μ g/kg) was given by intra-muscular injection to HFD-induced obese mice. The mice were killed 12 h after injection, and quadriceps muscle tissue was harvested. (A) The expression of PPAR α and p-AMPK protein was determined by Western blot. (B and C) Histograms show densitometry analysis of Western blots. Data are shown as the PPAR α / β -actin ratio or p-AMPK/total AMPK (tAMPK) ratio. β -actin was analyzed as a loading control. Data were normalized to total β -actin or AMPK. (D and E) Ex-4 (1 μ g/kg) was given by intra-muscular injection for 4 weeks to (D) HFD-induced obese mice or (E) regular chow-fed C57BL/6 mice. The mice were killed and soleus muscle tissue was harvested. The expression of UCP1 mRNA was determined by qRT-PCR. (F) Ex-4 (1 μ g/kg/day) was given by intra-muscular injection for 1 or 4 weeks to regular chow diet-fed C57BL/6 mice. After 1 week or 4 weeks later, the mice were killed and soleus muscle tissue was harvested. Soleus muscle lysates were immunoprecipitated (IP) with anti-UCP1 (14670, Cell Signaling) antibody and immunoblotted (IB) with anti-UCP1 (AB1426, Millipore) antibody. β -actin was a loading control. $n=4-5$, mean \pm S.E.M. # $P<0.05$, ## $P<0.01$, ### $P<0.001$ compared with untreated (Un) mice.

(Busiello *et al.* 2015). UCP1 has been known to be highly expressed in brown adipose tissue, but not in muscle (Ricquier & Bouillaud 2000). However, our results showed that the expression of UCP1 was significantly increased by Ex-4 treatment in differentiated C2C12 cells and mouse muscle. Recently, inducible brown adipocyte progenitors have been identified in skeletal muscle (Schulz *et al.* 2011, Murakami *et al.* 2015). It is not clear yet whether the increase of UCP1 expression by Ex-4 treatment is due to the effect on brown adipocyte progenitors or direct effect on muscle cells. Further studies are required to identify the detailed mechanisms. In addition, OCR was increased by Ex-4 treatment through uncoupling efficiency and proton leak in differentiated C2C12 cells. However, the expression of UCP2 and UCP3, which do not have a primary role in the regulation of energy metabolism (Schrauwen & Hesselink 2002), was not increased in differentiated C2C12 cells. Similarly, an increase of UCP1 expression by Ex-4 in differentiated brown adipocytes and brown adipose tissue of mice was also observed (Supplementary Figs 1 and 2,

see section on [supplementary data](#) given at the end of this article). The increased mRNA expression of the lipolytic enzyme, HSL, and the decreased FFA concentration by Ex-4 treatment in differentiated C2C12 cells, suggests that Ex-4 increases lipolysis and free fatty acid utilization, contributing to the activation of UCP-1.

β_3 -adrenergic receptors are thought to play a role in thermogenesis in brown fat and skeletal muscle, induce adaptive non-shivering thermogenesis and stimulate UCP1 expression (Golozoubova *et al.* 2006). We observed that the expression level of β_3 -adrenergic receptor mRNA was significantly increased by Ex-4 treatment. Taken together, induction of UCP1 and β_3 -adrenergic receptor expression by Ex-4 may contribute to the increase in energy expenditure through upregulation of non-shivering thermogenesis.

PPAR α is expressed predominantly in tissues that have a high level of fatty acid catabolism, such as liver, heart and muscle (Auboeuf *et al.* 1997). FXR, a member of nuclear receptor superfamily, is well known to regulate

lipid metabolism through improvement of fat oxidation (Prawitt *et al.* 2011), and FXR is involved in the induction of PPAR α . Our observation indicates that the GLP1 receptor agonist, Ex-4, significantly increased the expression of fatty acid oxidation-related genes such as PPAR α and FXR, which might contribute to increased fat oxidation and improve energy expenditure in C2C12 cells and muscle.

The presence of a GLP1 receptor in muscle is still controversial. Some studies have detected GLP1 receptor mRNA or protein, but others were studies that were unable to detect this receptor (Delgado *et al.* 1995, Bullock *et al.* 1996, Green *et al.* 2012). In our study, treatment with Ex-9, an antagonist of the GLP1 receptor, inhibited Ex-4-induced OCR and cAMP production was increased by Ex-4 treatment in C2C12 cells, indicating the presence of a GLP1 receptor in C2C12 cells. In addition, the increased expression of genes involved in thermogenesis and fat oxidation was inhibited by inhibitors of the cAMP-PKA pathways which are induced by the GLP1 receptor. Therefore, the Ex-4-mediated increases of OCR and thermogenic gene expression are likely due to the direct mechanism through the GLP1 receptor in muscle.

Recent studies have shown that AMPK activation was significantly associated with the improvement of insulin resistance. In addition, activation of skeletal muscle AMPK due to the overexpression of AMPK γ 3 increased fatty acid oxidation and protected against obesity (Barnes *et al.* 2004, Viollet *et al.* 2009). Furthermore, AMPK activity was increased by cold exposure in mouse brown adipose tissue (Mulligan *et al.* 2007). In this study, we found that the phosphorylated AMPK level was increased by Ex-4 in C2C12 cells and muscle suggesting that Ex-4 induced AMPK activation in muscle, which might contribute to the increase of energy expenditure and the improvement of insulin sensitivity. AMPK is known to be activated by liver kinase B1 (LKB1), Ca(2+)/calmodulin-dependent protein kinase kinase (CaMKK) or transforming growth factor- β -activated kinase 1 (TAK1) (Woods *et al.* 2005, Shackelford & Shaw 2009, Kim *et al.* 2012). As we observed that total intracellular ATP levels were increased by Ex-4 treatment in C2C12 cells, it is unlikely that AMPK activation was due to the increase of AMP/ATP or ADP/ATP ratios. Instead, it is possible that AMPK activation might be mediated in an AMP-independent manner such as by CaMKK activation. It was recently reported that a glucagon-like peptide-1 mimetic, increased intracellular Ca²⁺ and activated CaMKK β , which in turn activated AMPK in human aortic endothelial cells (Krasner *et al.* 2014).

To confirm the effects of Ex-4 in muscle *in vivo*, Ex-4 was given by intramuscular injection to

HFD-induced obese C57BL/6 mice or regular chow diet-fed C57BL/6 mice. HFD-induced obese models show impaired metabolic function, such as impaired AMPK activation (Ruderman & Prentki 2004). We found that the expression of UCP1, PPAR α and p-AMPK protein was significantly increased in Ex-4-injected mice compared with control mice. Thus, Ex-4 might improve energy expenditure in muscle both *in vitro* and *in vivo* through thermogenic gene regulation.

In conclusion, we investigated the effect of Ex-4 treatment on energy metabolism in muscle and found that treatment of Ex-4 increased lipid metabolism by enhancing fatty acid oxidation via upregulation of thermogenic genes such as UCP1, β_3 -adrenergic receptors, PPAR α , FXR and AMPK activation in muscle, which may contribute to reducing obesity and insulin resistance.

Supplementary data

This is linked to the online version of the paper at <http://dx.doi.org/10.1530/JME-16-0078>.

Declaration of interest

The authors declare that there is no conflict of interest that could be perceived as prejudicing the impartiality of the research reported.

Funding

This research was supported by grants from the Ministry of Health & Welfare, Republic of Korea (grant number: HI14C1135), and the Innovative Research Institute for Cell Therapy (A062260), the Korea Health Technology R&D Project through the Korea Health Industry Development Institute (KHIDI).

Author contribution statement

J-S Choung researched data and wrote the manuscript. Y-S Lee contributed to design of the study, researched data and wrote the manuscript. H-S Jun contributed to conception and design of the study and wrote the manuscript.

Acknowledgements

The authors thank Dr Ann Kyle for editorial assistance.

References

- Auboeuf D, Rieusset J, Fajas L, Vallier P, Frering V, Riou JP, Staels B, Auwerx J, Laville M & Vidal H 1997 Tissue distribution and quantification of the expression of mRNAs of peroxisome proliferator-activated receptors and liver X receptor-alpha in humans: no alteration in adipose tissue of obese and NIDDM patients. *Diabetes* **46** 1319–1327. (doi:10.2337/diab.46.8.1319)

- Bal NC, Maurya SK, Sopariwala DH, Sahoo SK, Gupta SC, Shaikh SA, Pant M, Rowland LA, Bombardier E, Goonasekera SA, *et al.* 2012 Sarcolipin is a newly identified regulator of muscle-based thermogenesis in mammals. *Nature Medicine* **18** 1575–1579. (doi:10.1038/nm.2897)
- Barnes BR, Marklund S, Steiler TL, Walter M, Hjalms G, Amarger V, Mahlapuu M, Leng Y, Johansson C, Galuska D, *et al.* 2004 The 5'-AMP-activated protein kinase gamma3 isoform has a key role in carbohydrate and lipid metabolism in glycolytic skeletal muscle. *Journal of Biological Chemistry* **279** 38441–38447. (doi:10.1074/jbc.M405533200)
- Briyal S, Shah S & Gulati A 2014 Neuroprotective and anti-apoptotic effects of liraglutide in the rat brain following focal cerebral ischemia. *Neuroscience* **281C** 269–281. (doi:10.1016/j.neuroscience.2014.09.064)
- Bullock BP, Heller RS & Habener JF 1996 Tissue distribution of messenger ribonucleic acid encoding the rat glucagon-like peptide-1 receptor. *Endocrinology* **137** 2968–2978. (doi:10.1210/en.137.7.2968)
- Busiello RA, Savarese S & Lombardi A 2015 Mitochondrial uncoupling proteins and energy metabolism. *Frontiers in Physiology* **6** 36. (doi:10.3389/fphys.2015.00036)
- Cechi K, Carpentier AC & Richard D 2013 Understanding the brown adipocyte as a contributor to energy homeostasis. *Trends in Endocrinology and Metabolism* **24** 408–420. (doi:10.1016/j.tem.2013.04.002)
- Choudhury Y, Yang Z, Ahmad I, Nixon C, Salt IP & Leung HY 2014 AMP-activated protein kinase (AMPK) as a potential therapeutic target independent of PI3K/Akt signaling in prostate cancer. *Oncoscience* **1** 446–456. (doi:10.18632/oncoscience.49)
- Corpeleijn E, Saris WH & Blaak EE 2009 Metabolic flexibility in the development of insulin resistance and type 2 diabetes: effects of lifestyle. *Obesity Reviews* **10** 178–193. (doi:10.1111/j.1467-789X.2008.00544.x)
- Delgado E, Luque MA, Alcantara A, Trapote MA, Clemente F, Galera C, Valverde I & Villanueva-Penacarrillo ML 1995 Glucagon-like peptide-1 binding to rat skeletal muscle. *Peptides* **16** 225–229. (doi:10.1016/0196-9781(94)00175-8)
- Ding X, Saxena NK, Lin S, Gupta NA & Anania FA 2006 Exendin-4, a glucagon-like protein-1 (GLP-1) receptor agonist, reverses hepatic steatosis in ob/ob mice. *Hepatology* **43** 173–181. (doi:10.1002/hep.21006)
- Drucker DJ 2006 The biology of incretin hormones. *Cell Metabolism* **3** 153–165. (doi:10.1016/j.cmet.2006.01.004)
- Fisler JS & Warden CH 2006 Uncoupling proteins, dietary fat and the metabolic syndrome. *Nutrition and Metabolism* **3** 38. (doi:10.1186/1743-7075-3-38)
- Golozubova V, Cannon B & Nedergaard J 2006 UCP1 is essential for adaptive adrenergic nonshivering thermogenesis. *American Journal of Physiology: Endocrinology and Metabolism* **291** E350–E357. (doi:10.1152/ajpendo.00387.2005)
- Green CJ, Henriksen TI, Pedersen BK & Solomon TP 2012 Glucagon like peptide-1-induced glucose metabolism in differentiated human muscle satellite cells is attenuated by hyperglycemia. *PLoS ONE* **7** e44284. (doi:10.1371/journal.pone.0044284)
- Hagen T & Lowell BB 2000 Chimeric proteins between UCP1 and UCP3: the middle third of UCP1 is necessary and sufficient for activation by fatty acids. *Biochemical and Biophysical Research Communications* **276** 642–648. (doi:10.1006/bbrc.2000.3535)
- Hwa JJ, Ghibaudi L, Williams P, Witten MB, Tedesco R & Strader CD 1998 Differential effects of intracerebroventricular glucagon-like peptide-1 on feeding and energy expenditure regulation. *Peptides* **19** 869–875. (doi:10.1016/S0196-9781(98)00033-3)
- Kim SY, Jeong S, Jung E, Baik KH, Chang MH, Kim SA, Shim JH, Chun E & Lee KY 2012 AMP-activated protein kinase- α 1 as an activating kinase of TGF- β -activated kinase 1 has a key role in inflammatory signals. *Cell Death Disease* **3** e357. (doi:10.1038/cddis.2012.95)
- Krasner NM, Ido Y, Ruderman NB & Cacicedo JM 2014 Glucagon-like peptide-1 (GLP-1) analog liraglutide inhibits endothelial cell inflammation through a calcium and AMPK dependent mechanism. *PLoS ONE* **9** e97554. (doi:10.1371/journal.pone.0097554)
- Layer P, Holst JJ, Grandt D & Goebell H 1995 Ileal release of glucagon-like peptide-1 (GLP-1). Association with inhibition of gastric acid secretion in humans. *Digestive Diseases and Sciences* **40** 1074–1082. (doi:10.1007/BF02064202)
- Lee YS & Jun HS 2014 Anti-diabetic actions of glucagon-like peptide-1 on pancreatic beta-cells. *Metabolism* **63** 9–19. (doi:10.1016/j.metabol.2013.09.010)
- Lee YS, Park MS, Choung JS, Kim SS, Oh HH, Choi CS, Ha SY, Kang Y, Kim Y & Jun HS 2012 Glucagon-like peptide-1 inhibits adipose tissue macrophage infiltration and inflammation in an obese mouse model of diabetes. *Diabetologia* **55** 2456–2468. (doi:10.1007/s00125-012-2592-3)
- Liu Q, Adams L, Broyde A, Fernandez R, Baron AD & Parkes DG 2010 The exenatide analogue AC3174 attenuates hypertension, insulin resistance, and renal dysfunction in Dahl salt-sensitive rats. *Cardiovascular Diabetology* **9** 32. (doi:10.1186/1475-2840-9-32)
- Lockie SH, Heppner KM, Chaudhary N, Chabenne JR, Morgan DA, Veyrat-Durebex C, Ananthakrishnan G, Rohner-Jeanrenaud F, Drucker DJ, DiMarchi R, *et al.* 2012 Direct control of brown adipose tissue thermogenesis by central nervous system glucagon-like peptide-1 receptor signaling. *Diabetes* **61** 2753–2762. (doi:10.2337/db11-1556)
- Mattsson CL, Csikasz RI, Chernogubova E, Yamamoto DL, Hogberg HT, Amri EZ, Hutchinson DS & Bengtsson T 2011 beta(1)-Adrenergic receptors increase UCP1 in human MADS brown adipocytes and rescue cold-acclimated beta(3)-adrenergic receptor-knockout mice via nonshivering thermogenesis. *American Journal of Physiology: Endocrinology and Metabolism* **301** E1108–E1118. (doi:10.1152/ajpendo.00085.2011)
- Mulligan JD, Gonzalez AA, Stewart AM, Carey HV & Saupé KW 2007 Upregulation of AMPK during cold exposure occurs via distinct mechanisms in brown and white adipose tissue of the mouse. *Journal of Physiology* **580** 677–684. (doi:10.1113/jphysiol.2007.128652)
- Murakami Y, Ojima-Kato T, Saburi W, Mori H, Matsui H, Tanabe S & Suzuki T 2015 Supplemental epilactose prevents metabolic disorders through uncoupling protein-1 induction in the skeletal muscle of mice fed high-fat diets. *British Journal of Nutrition* **114** 1774–1783. (doi:10.1017/S0007114515003505)
- Prawitt J, Abdelkarim M, Stroevé JH, Popescu I, Duez H, Velagapudi VR, Dumont J, Bouchaert E, van Dijk TH, Lucas A, *et al.* 2011 Farnesoid X receptor deficiency improves glucose homeostasis in mouse models of obesity. *Diabetes* **60** 1861–1871. (doi:10.2337/db11-0030)
- Ricquier D & Bouillaud F 2000 The uncoupling protein homologues: UCP1, UCP2, UCP3, StUCP and AtUCP. *Biochemical Journal* **345** 161–179. (doi:10.1042/bj3450161)
- Ruderman N & Prentki M 2004 AMP kinase and malonyl-CoA: targets for therapy of the metabolic syndrome. *Nature Reviews Drug Discovery* **3** 340–351. (doi:10.1038/nrd1344)
- Schrauwen P & Hesselink M 2002 UCP2 and UCP3 in muscle controlling body metabolism. *Journal of Experimental Biology* **205** 2275–2285.
- Schuh RA, Jackson KC, Khairallah RJ, Ward CW & Spangenburg EE 2012 Measuring mitochondrial respiration in intact single muscle fibers. *American Journal of Physiology: Regulatory, Integrative and Comparative Physiology* **302** R712–R719. (doi:10.1152/ajpregu.00229.2011)
- Schulz TJ, Huang TL, Tran TT, Zhang H, Townsend KL, Shadrach JL, Cerletti M, McDougall LE, Giorgadze N, Tchkonina T, *et al.* 2011 Identification of inducible brown adipocyte progenitors residing in skeletal muscle and white fat. *PNAS* **108** 143–148. (doi:10.1073/pnas.1010929108)

- Shackelford DB & Shaw RJ 2009 The LKB1-AMPK pathway: metabolism and growth control in tumour suppression. *Nature Reviews Cancer* **9** 563–575. (doi:10.1038/nrc2676)
- Shalev A, Holst JJ & Keller U 1997 Effects of glucagon-like peptide 1 (7–36 amide) on whole-body protein metabolism in healthy man. *European Journal of Clinical Investigation* **27** 10–16. (doi:10.1046/j.1365-2362.1997.540613.x)
- Terrien J, Ambid L, Nibbelink M, Saint-Charles A & Aujard F 2010 Non-shivering thermogenesis activation and maintenance in the aging gray mouse lemur (*Microcebus murinus*). *Experimental Gerontology* **45** 442–448. (doi:10.1016/j.exger.2010.03.013)
- Viollet B, Lantier L, Devin-Leclerc J, Hebrard S, Amouyal C, Mounier R, Foretz M & Andreelli F 2009 Targeting the AMPK pathway for the treatment of type 2 diabetes. *Frontiers in Bioscience* **14** 3380–3400. (doi:10.2741/3460)
- Winder WW & Hardie DG 1999 AMP-activated protein kinase, a metabolic master switch: possible roles in type 2 diabetes. *American Journal of Physiology* **277** E1–E10.
- Woods A, Dickerson K, Heath R, Hong SP, Momcilovic M, Johnstone SR, Carlson M & Carling D 2005 Ca²⁺/calmodulin-dependent protein kinase kinase-beta acts upstream of AMP-activated protein kinase in mammalian cells. *Cell Metabolism* **2** 21–33. (doi:10.1016/j.cmet.2005.06.005)

Received in final form 16 November 2016

Accepted 21 November 2016

Accepted Preprint published online 21 November 2016